

Band-Notched Small Slot Antenna Based on Time-Domain Reflectometry Modeling for UWB Applications

N. Mikaeilvand¹, M. Ojaroudi², and N. Ghadimi²

¹Department of Mathematics
Ardabil Branch, Islamic Azad University, Ardabil, Iran

²Young Researchers and Elite Club
Ardabil Branch, Islamic Azad University, Ardabil, Iran

Abstract — A design of a compact band-notched slot antenna by using defected structures with time domain designing method for UWB applications is presented. By cutting two modified meander line slots in the ground plane, a new resonance at the higher frequencies is excited, and hence, much wider impedance bandwidth can be produced that provides an ultra-wideband (UWB) frequency range. To generate a band-notched characteristic, we use the step-impedance resonator (SIR) slot at feed-line which contains a rectangular slot with a W-shaped strip protruded inside the slot. The proposed antenna can operate from 3.07 to 12.91 GHz with frequency band-notched function in 5.12-5.96 GHz to avoid interference from WLAN systems. To verify the validation of the proposed antenna, the equivalent circuit based on time domain reflectometry (TDR) analysis is presented. The proposed antenna exhibits almost omnidirectional radiation patterns in UWB frequency range. The designed antenna has a small size of 20×20 mm².

Index Terms — Defected transmission line, microstrip slot antenna, time-domain modeling.

I. INTRODUCTION

Commercial UWB systems require small low-cost antennas with omni-directional radiation patterns and large bandwidth [1]. It is a well-known fact that planar slot antennas present really appealing physical features, such as simple structure, small size and low cost. Due to all these interesting characteristics, planar slots are extremely attractive to be used in emerging UWB applications and growing research activity is being focused on them [2]-[3], and automatic design methods have been developed to achieve the optimum planar shape [4]-[6]. The wide frequency range for UWB systems between 3.1 to 10.6 GHz will cause interference to the existing wireless communication systems, such as the local area network (WLAN) for IEEE 802.11a which operates in 5.15-5.35 GHz and 5.725-5.825 GHz bands. Therefore, in order to eliminate this unwanted

interference, UWB antenna with band notch function is required. Several planar antennas with band notch characteristics have recently been presented. The easiest and most common technique is embedding a narrow slot into the radiating patch of the antenna and change the current flows on it, as used in [7]-[9]. In [7], different shapes of the slots (i.e., square ring and folded trapezoid) are used to obtain the band notch function. On the other hand, another method to avoid this frequency interference is the use of reconfigurable antennas. In [8], RF MEMS are used for notching the WLAN band while in [9], PIN diodes are used for the same reason.

In this paper, a simple method for designing a novel and compact microstrip-fed slot antenna with band-stop performance and time domain reflectometry analysis for UWB applications has been presented. In the presented antenna, based on defected ground structures (DGS) for bandwidth enhancement we use a pair of meander line slots in the ground plane and also based on defected microstrip structures (DMS), to generate a band-stop performance a rectangular slot with a W-shaped strip protruded inside the slot was inserted at feed-line [6]. Unlike other band-notched UWB antennas reported in the literature to date [3-6], this structure has an ordinary square radiating stub configuration. We also report their circuit models based on TDR analysis. The size of the designed antenna is smaller than the UWB antennas with band-notched function reported recently [3]-[9]. Simulated and measured results are presented to validate the usefulness of the proposed antenna structure for UWB applications.

II. ANTENNA DESIGN AND CONFIGURATION

The square slot antenna fed by a 50Ω microstrip line is shown in Fig. 1, which is printed on a FR4 substrate of width $W_{sub} = 20$ mm and length $L_{sub} = 20$ mm, thickness 0.8 mm, permittivity 4.4, and loss tangent 0.018. The proposed antenna is connected to a 50Ω

SMA connector for signal transmission. In this structure, by cutting the two meander line slots of suitable at the ground plane, it is found that much enhanced impedance bandwidth can be achieved for the proposed antenna. Regarding defected ground structures, the creating slots in the ground plane provide an additional current path. The DGS applied to a microstrip line causes a resonant character of the structure transmission with a resonant frequency controllable by changing the shape and size of the slot [10]. In addition, the defected microstrip structure (DMS) is playing an important role in the band-stop characteristic of this antenna, because it can adjust the electromagnetic coupling effects between the radiating stub and the ground plane. This phenomenon occurs because, with the use of a defected structure in transmission line distance, additional coupling is introduced between the bottom edge of the square radiating stub and the ground plane [9] and creates a band rejection around 5.12-5.96 GHz.

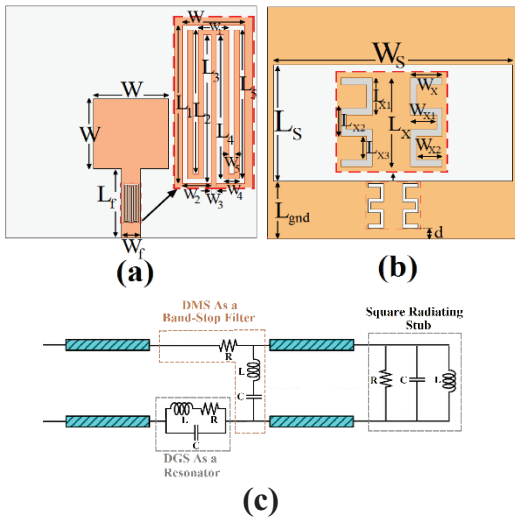


Fig. 1. Geometry of the proposed slot antenna with defected structures: (a) top layer, (b) bottom layer, and (c) the proposed antenna equivalent circuit model.

The final dimensions of the defected structures are as follows: $W_x = 1.25\text{mm}$, $L_x = 3.8\text{mm}$, $W_{x1} = 1.05\text{mm}$, $L_{x1} = 1.6\text{mm}$, $W_{x2} = 1\text{mm}$, $L_{x2} = 1.2\text{mm}$, $L_{x3} = 1\text{mm}$, $W = 1.2\text{mm}$, $L_1 = 3.3\text{mm}$, $W_1 = 0.6\text{mm}$, $L_2 = 3\text{mm}$, $W_2 = 0.55\text{mm}$, $L_3 = 3.1\text{mm}$, $W_3 = 0.1\text{mm}$, $L_4 = 1.1\text{mm}$, $W_4 = 0.3\text{mm}$, $L_5 = 1.1\text{mm}$, and $W_5 = 0.1\text{mm}$.

III. DEFECTED TRANSMISSION LINE

A. Defected structures (DGS and DMS) and its equivalent circuit models

Recently, the defected ground plane structures (DGS) and defected microstrip structure (DMS) have

been proposed for suppression of spurious response in the microstrip structures [11]-[12]. The proposed DGS and DMS with their equivalent circuit models are shown in Figs. 2 and 3, respectively. These defected structure on the ground plane and feed-line will perturb the incident and return current and induce a voltage difference on the ground plane and microstrip feed-line. These two effects can be modeled as a parallel LC circuit [12]. The resistance in equivalent circuits represents the loss of the slot and slit, which is small in general [13].

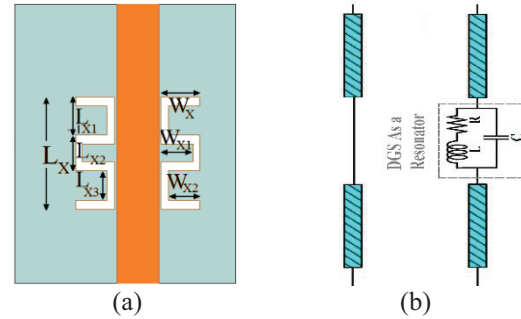


Fig. 2. (a) Geometry of the proposed defected ground structure (DGS), and (b) equivalent circuit model.

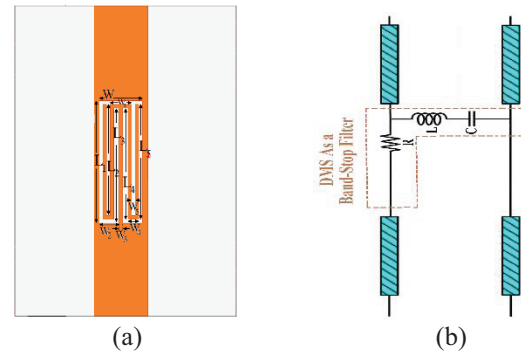


Fig. 3. (a) Geometry of the proposed defected microstrip structure (DMS), and (b) equivalent circuit model.

B. Time domain reflectometry analysis

In this section, the proposed defected structures with mentioned design parameters were simulated, and the TDR results of the input impedance for them in equivalent circuit and full-wave analysis cases are presented and discussed. The simulated full-wave TDR results are obtained using the Ansoft simulation software high-frequency structure simulator (HFSS) [14].

In order to calculate of the TDR results for the proposed equivalent circuits, the impedance of these circuits in Laplace domain can be represented as (1) and (2):

$$Z_{DGS} = \frac{Ls + R}{LCs^2 + RCs + 1}, \quad (1)$$

$$Z_{DMS} = \frac{LCs^2 + RCs + 1}{Cs}. \quad (2)$$

Assume that the characteristic impedance of the microstrip line is Z_0 , we can write the reflection coefficient through defected structures as (3) which is observed at the source end, i.e., Port 1:

$$\Gamma_z(s) = \frac{Z(s)}{Z(s) + 2Z_0}, \quad (3)$$

where $Z(s)$ is defected structures impedance as shown in (1) and (2), and Z_0 is equal to 50Ω . Therefore, the reflected waveform for the proposed DGS and DMS can be written as:

$$\Gamma_{DGS}(s) = \frac{Ls + R}{2Z_0LCs^2 + (2Z_0RC + L)s + R + 2Z_0}, \quad (4)$$

$$\Gamma_{DMS}(s) = \frac{LCs^2 + RCs + 1}{LCs^2 + (R + 2Z_0)Cs + 1}. \quad (5)$$

A step voltage source with rise time τ_r and amplitude V_0 , can be expressed as [13]:

$$V_{in}(s) = \frac{V_0}{2\tau_r} \frac{1}{s^2} (1 - e^{-\tau_r s}). \quad (6)$$

Therefore, the reflected waveform in Laplace domain can be written as:

$$V_{TDR}(s) = V_{in}(s) \Gamma_{DGS, DMS}(s). \quad (7)$$

In TDR measurements, the impedance follows from:

$$Z_{TDR} = Z_0 \times (V_{in}(t) + V_{TDR}(t)) / (V_{in}(t) - V_{TDR}(t)), \quad (8)$$

where Z_0 is the characteristic impedance of the transmission line at the terminal.

Figures 4 and 5 show the simulated reflection waveforms observed at port 1 of the defected structures, as shown in Fig. 2 and Fig. 3, and with a 50Ω termination on port 2. The excitation source is a step wave with amplitude 1 Volt and rise time of 30 psec. The corresponding result predicted by the equivalent circuit model is also shown in these figures. As shown in Figs. 4 and 5, TDR curves have started with impedance just under 50Ω . At impedance discontinuities, part of the input signal is reflected. These reflections, after traveling back, reach terminal Port 1 and are observed there [15]. We computed the values of the L, R and C of the proposed equivalent circuits, by fitting the TDR curves of equivalent circuit (RLC circuit) with the TDR curves of DGS/DMS, by proposing two equivalent circuit models we can try to tune the parameters of the circuit elements in the models so that time domain response from theoretical analysis match. The optimal dimensions of the equivalent circuit models parameters are specified in Table 1.

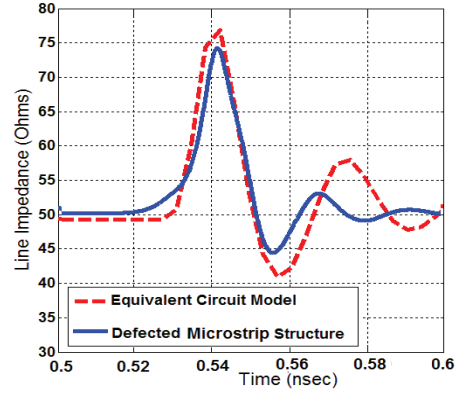


Fig. 4. The reflected waveforms simulated by HFSS and predicted by equivalent circuit model, and the proposed defected microstrip structure shown in Fig. 2.

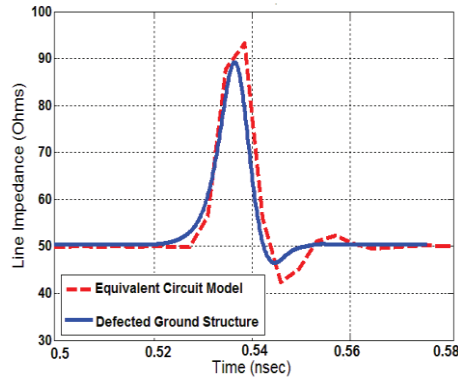


Fig. 5. The reflected waveforms simulated by HFSS and predicted by equivalent circuit model, and the proposed defected ground structure shown in Fig. 3.

Table 1: Equivalent circuit model parameters

Element	DMS	DGS
L	2.8 (nH)	1.6 (nH)
C	6.1 (pF)	17.75 (pF)
R	0.532 (Ω)	0.73 (Ω)

IV. RESULTS AND DISCUSSIONS

The planar slot antenna with various design parameters were constructed, and the numerical and experimental results of the input impedance and radiation characteristics are presented and discussed. The parameters of this proposed antenna are studied by changing one parameter at a time and fixing the others.

Figure 6 shows the structure of the various antennas used for simulation studies. Return loss characteristics for ordinary square slot antenna (Fig. 6 (a)), with two modified W-shaped slots with variable dimensions on the ground plane (Fig. 6 (b)), and with two modified

meander line slots with variable dimensions on the ground plane and a protruded W-shaped strip inside rectangular slot on the feed-line (Fig. 6 (c)), are compared in Fig. 7. As shown in Fig. 7, it is observed that the upper frequency bandwidth is affected by using the modified meander line slots in the ground plane and notched frequency bandwidth is sensitive to the protruded W-shaped strip inside rectangular slot on the feed-line.

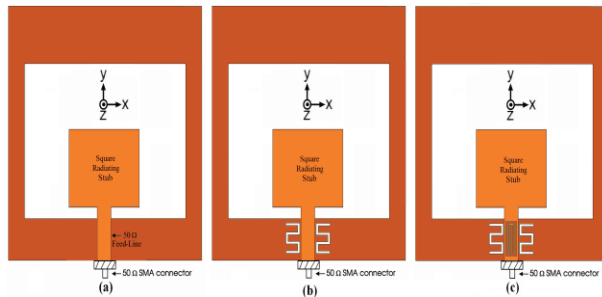


Fig. 6. (a) The ordinary square slot antenna, (b) the square antenna with two modified W-shaped slots on the ground plane (DGS), and (c) the square antenna with two modified meander line slots on the ground plane and a protruded W-shaped strip inside rectangular slot on the feed-line (DGS and DMS).

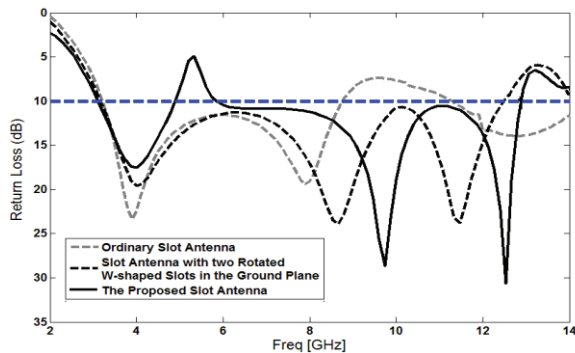


Fig. 7. Simulated return loss characteristics for antennas shown in Fig. 6.

As shown in Fig. 7, in the proposed antenna configuration, the ordinary square slot can provide the fundamental and next higher resonant radiation band at 4.12 and 8.18 GHz, respectively, in the absence of these defected structures. The upper frequency bandwidth is significantly affected by using the meander line slots on the ground plane. This behavior is mainly due to the change of surface current path by the dimensions of meander line slots at third resonance frequency (12.65 GHz), as shown in Fig. 8 (a). In addition, by inserting the protruded W-shaped strip inside rectangular slot with variable dimensions on the feed-line, a band notched function is created [6]. Figure 8 (b) presents the

simulated current distributions on the radiating stub and feed-line at the notched frequency (5.5 GHz). As shown in Fig. 8 (b), at the notched frequency the current flows are more dominant around of the protruded W-shaped strip inside rectangular slot at feed-line.

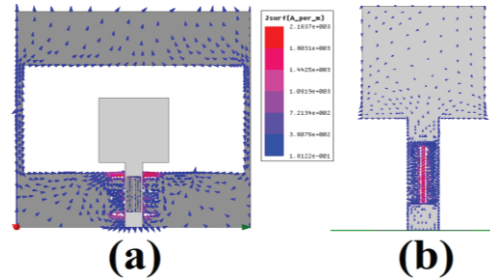


Fig. 8. Simulated surface current distributions plane for the proposed slot antenna: (a) on the ground at the third resonance frequency (12.65 GHz), and (b) on the radiating stub at notch frequency (5.5 GHz).

In order to increase the upper frequency bandwidth, two meander-line slots are inserted in the ground plane of the proposed antenna, as displayed in Fig. 1. To investigate the effects of meander-line slots size on the proposed antenna, the simulated return curves with different values of meander-line slots lengths are plotted in Fig. 9. It is found that by inserting the meander line slots with suitable dimensions in the ground plane additional resonance is excited, and hence, much wider impedance bandwidth with multi-resonance characteristics can be produced, especially at the higher frequencies.

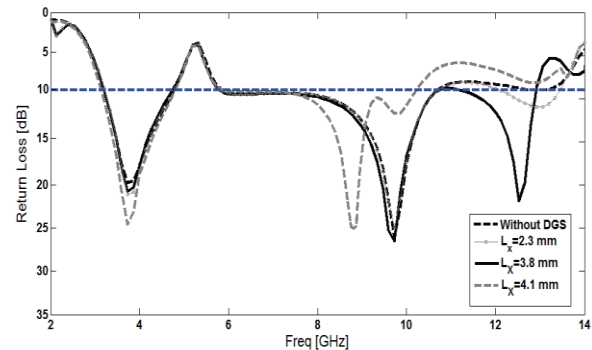


Fig. 9. Simulated return loss characteristics of the proposed antenna with different values of L_x .

In order to generate band notched performance, a protruded W-shaped strip inside rectangular slot is inserted in the microstrip feed line of the proposed antenna, as displayed in Fig. 1. Four such structures with different sizes are specified in Table 2 as cases 1, 2, 3 and 4.

Table 2: Four cases of proposed antenna with different values of protruded W-shaped strip

Parameter	W (mm)	L ₁ (mm)	W ₂ (mm)	L ₃ (mm)
Case I	1	2.8	0.5	2.5
Case II	1.2	3.3	0.55	3.1
Case III	1.4	3.3	0.6	3.3
Case IV	1.25	3.8	0.65	3.6

Figure 10 shows the effects of protruded W-shaped strip with different values on VSWR characteristics. From these results, we can conclude that the notch frequency is controllable by changing the protruded W-shaped strip length.

The proposed antenna with optimal design, as shown in Fig. 11, was built and tested. Figure 12 shows the measured and simulated return loss characteristics of the proposed antenna. The fabricated antenna has the frequency band of 3.06 to over 14.27 GHz. As shown in Fig. 12, there exists a discrepancy between measured data and the simulated results. This discrepancy is mostly due to a number of parameters, such as the fabricated antenna dimensions as well as the thickness and dielectric constant of the substrate on which the antenna is fabricated, the wide range of simulation frequencies.

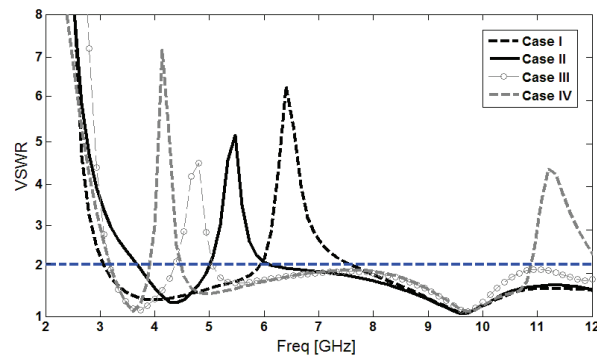


Fig. 10. Simulated VSWR characteristics for the proposed antenna with four cases 1, 2, 3 and 4 as shown in Table 2.

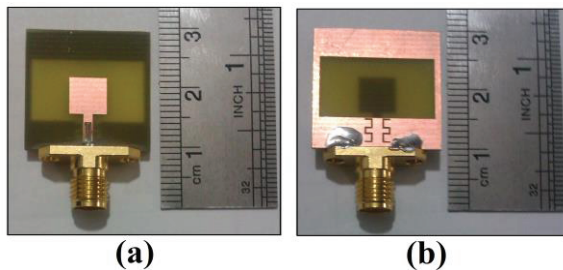


Fig. 11. Photograph of the realized printed square slot antenna.

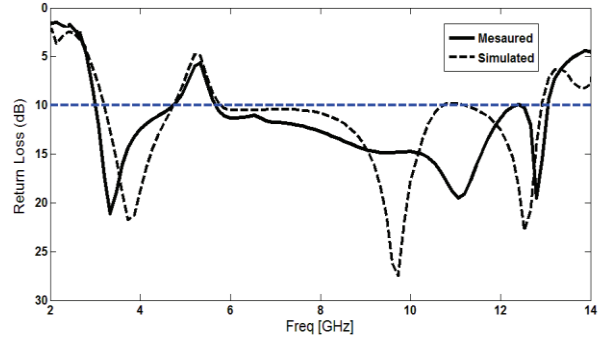


Fig. 12. Measured and simulated return loss for the proposed antenna.

Figure 13 shows the measured radiation patterns including the *H*-plane (*x-z* plane) and *E*-plane (*y-z* plane). The main purpose of the radiation patterns is to demonstrate that the antenna actually radiates over a wide frequency band. It can be seen that the radiation patterns in *x-z* plane are nearly omni-directional for the four frequencies.

Figure 14 shows the measured and simulated maximum gain for the proposed. A two-antenna technique is used to measure the radiation gain in the *z* axis direction (*x-z* plane). It can be observed in Fig. 14, that by using defected ground and defected microstrip structures, a sharp decrease of maximum gain in the notched frequency band at 5.5 GHz are shown. Also, as shown in Fig. 14, the measured results agree very well with the simulated results in the desired frequencies.

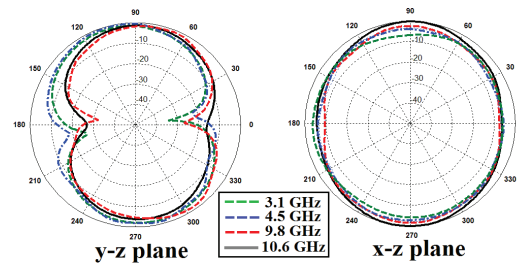


Fig. 13. Measured radiation patterns of the proposed antenna.

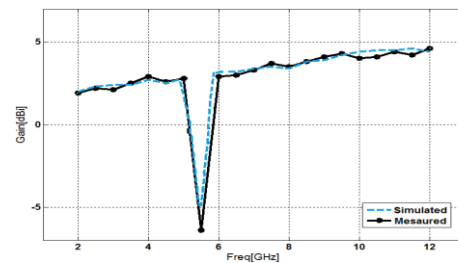


Fig. 14. Measured and simulated maximum gain for the proposed antenna in the *z* axis direction (*x-z* plane).

V. CONCLUSION

In this paper, a novel compact printed slot antenna (PSA) with band notched function and a novel time domain method to extract the equivalent RLC of the defected structures has been proposed for UWB applications. The analytic formulations for the equivalent circuit model are obtained based on time-domain reflectometry theory, Laplace transform. The fabricated antenna covers the frequency range for UWB systems between 3.07 to 12.91 GHz with band-notched characteristic around 5.12 to 5.96 GHz to avoid interference from WLAN systems. Experimental results show that the proposed antenna could be a good candidate for UWB application.

REFERENCES

- [1] H. Schantz, *The Art and Science of Ultra Wideband Antennas*, Artech House, 2005.
- [2] M. Ojaroudi and A. Faramarzi, "Multi-resonance small square slot antenna for ultra-wideband applications," *Microwave and Optical Tech. Letters*, vol. 53, no. 9, Sept. 2011.
- [3] A. Dastranj, A. Imani, and M. Naser-Moghaddasi, "Printed wide-slot antenna for wideband applications," *IEEE Transactions on Antenna and Propagations*, vol. 56, no. 10, pp. 3097-3102, Oct. 2008.
- [4] M. Ojaroudi, G. Kohneshahri, and J. Noory, "Small modified monopole antenna for UWB application," *IET Microw, Antennas Propag.*, vol. 3, no. 5, pp. 863-869, Aug. 2009.
- [5] R. Rouhi, C. Ghobadi, J. Nourinia, and M. Ojaroudi, "Ultra-wideband small square monopole antenna with band notched function," *Microwave and Optical Tech. Letters*, vol. 52, no. 8, Aug. 2010.
- [6] M. Ojaroudi, H. Ebrahimian, C. Ghobadi, and J. Nourinia, "Small microstrip-fed monopole printed monopole antenna for UWB applications," *Microwave and Optical Tech. Letters*, vol. 52, no. 8, Aug. 2010.
- [7] W. J. Lui, C. H. Cheng, Y. Cheng, et al., "Frequency notched ultra wideband microstrip slot antenna with a fractal tuning stub," *Electronic Letters*, no. 41, pp. 294-296, 2005.
- [8] S. Nikolaou, N. D. Kingsley, G. E. Ponchak, J. Papapolymerou, and M. M. Tentzeris, "UWB elliptical monopoles with a reconfigurable band notch using MEMS switches actuated without bias lines," *IEEE Transactions on Antenna and Propagation*, vol. 57, no. 8, pp. 2242-2251, Aug. 2009.
- [9] A. Valizade, C. Ghobadi, J. Nourinia, and M. Ojaroudi, "A novel design of reconfigurable slot antenna with switchable band notch and multiresonance functions for UWB applications," *IEEE Antennas and Wireless Propagation Letters*, vol. 11, no. 1, pp. 1166-1169, 2012.
- [10] H. D. Chen, H. M. Chen, and W. S. Chen, "Planar CPW-fed sleeve monopole antenna for ultra-wideband operation," *IET Microw, Antennas Propag.*, vol. 152, no. 6, pp. 491-494, Dec. 2005.
- [11] A. B. Abdel-Rahman, A. K. Verma, A. Boutejdar, and A. S. Omar, "Control of bandstop response of hi-lo microstrip low-pass filter using slot in ground plane," *IEEE Trans. Microw. Theory Tech.*, vol. 52, no. 3, pp. 1008-1013, Mar. 2004.
- [12] C. H. Cheng, C. H. Tsai, and T. L. Wu, "A novel time domain method to extract equivalent circuit model of patterned ground structures," *IEEE Microw. Wireless Compon. Lett.*, vol. 17, no. 11, Nov. 2010.
- [13] M. Ojaroudi, N. Ojaroudi, and Y. Ebazadeh, "Dual band-notch small square monopole antenna with enhanced bandwidth characteristics for UWB applications," *ACES Journal*, vol. 27, no. 5, pp. 420-426, May 2012.
- [14] Ansoft High Frequency Structure Simulation (HFSS), ver. 13, Ansoft Corporation, 2011.
- [15] Z. Chen, X. Wu, H. Li, N. Yang, and M. Y. W. Chia, "Considerations for source pulses and antennas in UWB radio systems," *IEEE Trans. Antennas Propag.*, vol. 52, no. 7, pp. 1739-1748, Jul. 2004.